Acta Pharmacologica Sinica

www.nature.com/aps

ARTICLE

A thienopyridine, CB-20, exerts diuretic activity by inhibiting urea transporters

Min Li[1], Yan Zhao[2,3], Shun Zhang[1], Yue Xu[1], Shu-yuan Wang[1], Bo-wen Li[2], Jian-hua Ran[4], Run-tao Li[2] and Bao-xue Yang[1]

Urea transporters (UTs) are transmembrane proteins selectively permeable to urea and play an important role in urine concentration. UT-knockout mice exhibit the urea-selective urine-concentrating defect, without affecting electrolyte balance, suggesting that UT-B inhibitors have the potential to be developed as novel diuretics. In this study, we characterized a novel compound 5-ethyl-2-methyl-3-amino-6-methylthieno[2,3-b]pyridine-2,5-dicarboxylate (CB-20) with UT inhibitory activity as novel diuretics with excellent pharmacological properties. This compound was discovered based on high-throughput virtual screening combined with the erythrocyte osmotic lysis assay. Selectivity of UT inhibitors was assayed using transwell chambers. Diuretic activity of the compound was examined in rats and mice using metabolic cages. Pharmacokinetic parameters were detected in rats using LC–MS/MS. Molecular docking was employed to predict the potential binding modes for the CB-20 with human UT-B. This compound dose-dependently inhibited UT-facilitated urea transport with IC_{50} values at low micromolar levels. It exhibited nearly equal inhibitory activity on both UT-A1 and UT-B. After subcutaneous administration of CB-20, the animals showed polyuria, without electrolyte imbalance and abnormal metabolism. CB-20 possessed a good absorption and rapid clearance in rat plasma. Administration of CB-20 for 5 days did not cause significant morphological abnormality in kidney or liver tissues of rats. Molecular docking showed that CB-20 was positioned near several residues in human UT-B, including Leu364, Val367, and so on. This study provides proof of evidence for the prominent diuretic activity of CB-20 by specifically inhibiting UTs. CB-20 or thienopyridine analogs may be developed as novel diuretics.

Keywords: diuretics; thienopyridine; urea transporter; electrolytes; drug discovery

Acta Pharmacologica Sinica (2020) 41:65–72; https://doi.org/10.1038/s41401-019-0245-5

INTRODUCTION

Diuretics are mainly used for the treatment of edema caused by various pathological processes by targeting the kidney [1, 2]. Furthermore, diuretics administered as a first-line drug alone or together with other antihypertensive drugs used to treat hypertension can reduce the incidence of cardiovascular and cerebrovascular complications and mortality. Traditional diuretics, such as loop diuretics and thiazide diuretics, specifically inhibit the $Na^+/K^+/2Cl^-$ cotransporters in the thick ascending limb and the Na^+/Cl^- cotransporters in the distal convoluted tubules, respectively. Then, by inhibiting NaCl reabsorption, the ability to concentrate urine is reduced, and a large amount of urine close to isosmotic conditions is excreted. Long-term use of these diuretic drugs can cause electrolyte disturbance, especially deficiency of blood potassium, which will seriously affect the normal physiological functions of the body, such as causing hyperglycemia, hyperlipidemia, arrhythmia, and even life-threatening complications. The clinical application of potassium-conserving diuretic drugs mainly includes drugs that function through aldosterone antagonistic activity in the collecting tube and a distal curved tubule, showing the effect of sodium and potassium conservation, and long-term use can cause hyperkalemia and other adverse reactions [3–8]. A V_2R antagonist discovered recently can specifically antagonize the combination of AVP and a receptor, thereby antagonizing the effects of AVP, such as hypertension and antidiuresis, to increase the amount of urine [9]. However, V_2R antagonists cause many side effects, such as thirst, urination, nocturnal urination, and liver injury. In addition, a rapid increase in blood sodium can be harmful and cause osmotic demyelination, resulting in dysarthria, mutism, dysphagia, lethargy, affective changes, spastic quadriparesis, seizures, coma, or death [10]. Therefore, we need to find and develop new diuretic drugs with minimal electrolyte disturbance and few side effects.

Urea transporters (UTs) play a very important role in urine concentration [11–14]. UTs are divided into two subgroups: UT-A and UT-B [15]. The UT-A subfamily has six isoforms: UT-A1 to UT-A6, which are encoded by a single gene, SLC14a2, by alternative splicing and promoters. UT-A1 and UT-A3 are expressed in the renal inner medullary collecting duct [16], UT-A2 is located in the thin descending limb, and UT-A4 mRNA is detected in the rat kidney medulla; however, endogenous expression of UT-A4 protein in the kidney has not been verified. UT-A5 is located in the testis and UT-A6 is located in the colon. UT-B, which is encoded by the gene SLC14a1, is primarily located in the

[1]State Key Laboratory of Natural and Biomimetic Drugs, Department of Pharmacology, School of Basic Medical Sciences, Peking University, Beijing 100191, China; [2]State Key Laboratory of Natural and Biomimetic Drugs, School of pharmaceutical Sciences, Peking University, Beijing 100191, China; [3]College of Pharmacy, Inner Mongolia Medical University, Hohhot 010110, China and [4]Chongqing Medical University, Chongqing 400016, China
Correspondence: Run-tao Li (lirt_1@163.com) or Bao-xue Yang (baoxue@bjmu.edu.cn)

Received: 14 February 2019 Accepted: 28 April 2019
Published online: 18 June 2019

descending vasa recta, as well as in a number of other tissues, including the heart, colon, testis, bladder, brain, and erythrocytes [17]. Previous studies found that selective knockout of UTs can block urea recycling in the kidney, thus reducing the urine concentration capacity of the kidney, and produce a urea-selective diuretic effect without affecting the excretion of Na^+, K^+, and Cl^- [11, 12, 14, 18–21]. Therefore, it is proposed that UT inhibitors can reduce the osmotic pressure gradient in the kidney by blocking urea recycling in the kidney, thus producing a diuretic effect. This diuretic mechanism does not interfere with the reabsorption and excretion of Na^+, K^+, and Cl^- in the kidney, so it may not cause a disturbance of the electrolyte balance in the body, which suggests that UT inhibitors might be novel diuretics that can cause the excretion of water without disturbing the electrolyte balance and metabolism [22–27].

Our previous study discovered a class of thienoquinolines that showed extensive UT inhibitory activity [28]. We optimized the compound with the core structure of thienoquinoline to obtain PU-14, which exhibited strong UT-B inhibitory activity in human, rat, and mouse erythrocytes with IC_{50} values at the micromolar level. Amazingly, after subcutaneous administration of PU-14 in rats, the urine output significantly increased in a dose-dependent manner. The urine output of the rats with long-term administration of PU-14 was significantly higher than that of the vehicle control rats. There was no obvious difference in the concentration of non-urea solutes between PU-14-treated and vehicle control rats, which suggests that PU-14 brings about urea-selective diuresis without disturbing electrolyte metabolism. Blood Na^+, K^+, Cl^-, urea, glucose, triglyceride, and total cholesterol levels did not change after 7 days of treatment with PU-14.

In this study, we aimed to evaluate a novel UT inhibitor, CB-20, whose core is thienopyridine, obtained when we modified and optimized the structure of the thienoquinolines using a High-throughput Virtual Screening (HTVS) model [29] and the erythrocyte osmotic lysis assay [30]. CB-20 exhibited good inhibitory activity in vitro and had inhibitory activity against both UT-A1 and UT-B. Moreover, subcutaneous administration of CB-20 can increase urine output in vivo without disturbing the electrolyte balance and normal metabolism. These findings indicate that CB-20 has the potential to be a candidate compound for novel diuretics targeting UTs.

MATERIALS AND METHODS

Animals

Male Sprague-Dawley (SD) rats at 8 weeks old were supplied by the Peking University Health Science Center (PUHSC) Laboratory Animal Service Center. Male UT-null mice and UT-B-null mice at 8 weeks of age on a C57BL/6J genetic background were generated as described previously [14, 18]. All animals were raised at room temperature and relative humidity with natural access to food and water. All animal experiments conformed to the Guide for the Care and Use of Laboratory Animals published by the US National Institutes of Health (NIH Publication, Eighth Edition, 2011) and were approved by the PUHSC Animal Experimentation Ethics Committee (Laboratory animal use license no. SYXK (JING) 2016-0041, Laboratory animal production license no. SCXK (JING) 2016-0010).

Collection of human, mouse, and rat blood

Vein blood was collected from humans, SD rats, wild-type mice, UT-B-null mice, and UT-null mice as reported previously [28].

Synthesis of CB-20

The compound CB-20 was synthesized by our laboratory as follows: all reagents and solvents were purchased from commercial sources and were used without further purification. Ethyl acetoacetate (1.302 g, 10 mM) and DMF–DMA (1.430 g, 12 mM) were dissolved in DCE (5 mL). The solution was refluxed for 8 h and then cooled to room temperature. The solvent was concentrated under vacuum to provide a red oil without further purification. NaOEt (0.34 g, 5 mM) was dissolved in EtOH (15 mL). 2-Cyanothioacetamide (0.46 g, 5.5 mM) was added slowly to the solution, followed by the red oil prepared above, in an ice-water bath. The resulting mixture was stirred overnight. The solvent was removed. Next, 1 N HCl was added to the residue to adjust the pH to 4. The mixture was stirred vigorously for an additional 2 h. Ethyl-5-cyano-2-methyl-6-thioxo-1,6-dihydropyridine-3-carboxylate was precipitated and collected by filtration as a yellow solid. The solid (0.93 g, 4.2 mM), DMF (20 mL), methyl chloroacetate (0.54 g, 5 mM), and 1.8 N KOH aqueous solution (2.7 mL) were mixed and stirred for 3 h at room temperature. Two hundred milliliters of water was added. The solid was filtered and recrystallized with petroleum ether/ethyl acetate to afford the title compound as a white crystal. Yield 32%. M.P.: 193–194 °C. ^{1}H NMR (400 MHz, $CDCl_3$) δ 8.51 (s, 1H), 6.05 (s, 2H), 4.43 (q, $J = 7.1$ Hz, 2H), 3.91 (s, 3H), 2.95 (s, 3H), and 1.44 (t, $J = 7.1$ Hz, 3H). ^{13}C NMR (101 MHz, $CDCl_3$) δ 166.18, 165.60, 162.93, 160.95, 146.42, 132.11, 123.11, 121.45, 98.17, 61.56, 51.75, 25.63, and 14.33. HRMS (ESI^+): *m/z* calcd. for $C_{13}H_{15}N_2O_4S$ $[M + H]^+$: 295.07470. Found: 295.07427. CB-20 was resolved and stored as a 10 mM solution in dimethyl sulfoxide (DMSO).

UT-B inhibitory activity identified by erythrocyte lysis

We used a high-throughput screening assay to identify UT-B inhibitors using erythrocytes [31]. Erythrocytes obtained from veins were diluted to a hematocrit value of 2% in hyperosmolar PBS containing 1.25 M urea and 5 mM glucose. Erythrocyte suspensions were kept at room temperature for 2 h with a periodic pipette mixture. Then, 99 µL of erythrocyte suspension was added to each well of a 96-well microplate, to which compounds being tested were then added (1 µL, 10 µM final compound concentration, 1% final DMSO concentration). After 6 min of incubation, 20 µL of the erythrocyte suspension was added rapidly to each well of a 96-well black-walled plate containing 180 µL of isomolar PBS containing 1% DMSO. A single time-point measure of the absorbance at 710 nm with a plate reader was used to quantify erythrocyte lysis [31]. The percentage of erythrocyte lysis in each well was calculated as follows: % lysis $= 100\% \times (A_{neg} - A_{test})/(A_{neg} - A_{pos})$, where A_{test} is the absorbance value from a test well. The positive control was the nonspecific UT-B inhibitor phloretin (Sigma-Aldrich, 700 µM final concentration).

Cell culture and cytotoxicity assay

Type I MDCK (Madin–Darby canine kidney) cells (ATCC no. CCL-34) were cultured in Dulbecco's modified Eagle's medium (Gibco) supplemented with 10% fetal bovine serum (HyClone) at 37 °C in a humidified 95% air/5% CO_2 atmosphere. MDCK cells (1×10^4 cells per 100 µL/well) were cultured in a 96-well plate. The cells were exposed to different concentrations of CB-20 for 72 h, when they grew to ~70% confluence. Then, 10 µM CCK-8 solution was added to each well and incubated for 1 h away from light, and the absorbance at 450 nm was measured. The experiment was repeated three times.

Assay of UT-facilitated urea flux

MDCK cells stably expressing human UT-A1 or UT-B were cultured in DMEM supplemented with 10% fetal bovine serum. To measure urea flux, cells were grown on 12-mm collagen-coated Costar Transwell inserts (0.4-µm pore size, Corning) for 4 days at 37 °C in the presence of 5% CO_2 when cells formed a tight monolayer (transepithelial resistance of 1 kΩ/cm^2). An assay of UT-facilitated urea flux was performed as previously described [28]. After removing the DMEM and washing with PBS, PBS containing forskolin (FSK) with or without CB-20 was added to both the

apical- and basal-facing surfaces. After 30 min of incubation, the basal-facing solution was replaced by PBS containing 15 mM urea with or without CB-20. Apical fluid samples were collected at 0, 1, 3, 5, 10, 15, 20, 30, 40, 50, and 60 min. The samples were subjected to an assay for urea (Quantichrome Urea Assay Kit; BioAssay Systems, Hayward, CA) according to the kit procedure. Then, the inhibition rate was calculated from the initial slope with GraphPad Prism 5. The experiment was repeated three times. The UT-B-facilitated urea flux assay was performed with the same procedure as the UT-A1-facilitated urea flux assay, except for FSK stimulation.

Measurement of diuretic activity of CB-20

Male SD rats (six rats/group, body weight 200–250 g), UT-B-null mice, and UT-null mice [14] (six mice/group, body weight 20–25 g) were allowed to acclimate to metabolic cages (Harvard Apparatus) for 4 days and fed with a standard synthetic rodent diet. Water and food were provided ad libitum during the whole study. The bladder of the rat or mouse was emptied by gentle abdominal massage. Then, urine was collected every 2 h. By subcutaneous injection, 25, 50, or 100 mg/kg CB-20 in 40% (g/mL) 2-hydroxypropyl-β-cyclodextrin was administered once. As a vehicle control, 40% 2-hydroxypropyl was used. Urinary volume was measured by gravimetry, which assumed a density of 1 g/mL. Urinary osmolality was measured by freezing-point depression (Micro-osmometer, Fisker Associates). Urea concentration was measured with a urea assay kit as described above.

To study the diuretic activity of multiple doses, 100 mg/kg CB-20 (the first dose was double) in 2-hydroxypropyl-β-cyclodextrin was administered by subcutaneous injection three times a day. Urine was collected, and water intake was recorded every 24 h. At 2.5 h after the final administration, the rats were anesthetized with 20% urethane, and blood samples were collected by renal artery puncture. Serum and urinary osmolality and urea concentration were measured as described above. Na^+, K^+, Cl^-, cholesterol (T-CHO), triglyceride (TG), high-density lipoprotein (HDL-C), and low-density lipoprotein (LDL-C) levels were measured in a clinical chemistry laboratory.

Histology

The rats were anesthetized with 20% urethane and fixed with 4% paraformaldehyde by heart perfusion. The kidneys and liver were fixed with formalin and embedded in paraformaldehyde, and 5-μm paraffin sections were cut and stained with hematoxylin and eosin.

Rat pharmacokinetics

Male SD rats (body weight 200–250 g) were fed with standard food and water at a stable temperature (22 ± 2 °C) and humidity (55% ± 5%) with a 12-h light–dark cycle. A 10.0 mg/mL CB-20 suspension reconstituted in 40% H-β-CD was administered at 100 mg/kg via the subcutaneous route. Blood samples (250 μL) were collected via tail vein puncture at 0.083, 0.25, 0.5, 1, 2, 4, 6, 8, 12, and 24 h in tubes with an anticoagulant, and plasma samples were obtained by centrifugation at 4000 r/min for 15 min. Calibration standards were prepared by spiking the working solution into untreated rat plasma to afford final concentrations of 1–2000 nM. These samples were analyzed by a high-performance liquid chromatography–tandem mass spectrometry (LC–MS/MS) system equipped with a Shimadzu LC-20AD pump and Shimadzu SIL-20AC autosampler (Shimadzu, Japan). Chromatographic separation was performed on a Kinetex 2.6-μm C18 100-Å column (30 mm × 3.00 mm, Phenomenex, CA, USA) at room temperature using a mobile phase of deionized water supplemented with 0.05% (v/v) formic acid (solvent A) and acetonitrile supplemented with 0.1% (v/v) formic acid (solvent B). The gradient was performed with a total flow of 0.7 mL/min as follows: 0–0.40 min, 30% (B), 0.40–2.00 min, 70%–95% (B), 2.00–2.20 min, 95% (B), 2.20–2.21 min, 95%–30% (B), and 2.21–3.00 min, 30% (B). Mass spectrometric analysis was carried out using a SCIEX Triple Quad™ 5500 mass spectrometer (Foster City, CA, USA) equipped with an electrospray ionization (ESI) interface in positive ionization mode. Quantification was achieved by multiple-reaction monitoring to identify the analyte (CB-20) and internal standard (terfenadine). The declustering potential (DP) and collision energy (CE) were optimized as follows: DP: 61 V and CE: 45 V for CB-20 and DP: 66 V and CE: 37 V for IS. The selected mass transitions were m/z 295.10 → 207.10 for CB-20 and m/z 472.40 → 436.40 for IS. Analyst Software 1.6.1 (SCIEX) was used for data acquisition and analysis.

Molecular docking

The human UT-B protein structure used in docking was downloaded from the Protein Data Bank (PDB: 6QD5), and the structure solved at 2.4 Å was downloaded from the RCSB PDB bank (https://www.rcsb.org/). The protein was prepared for docking using Protein Preparation (Maestro, Schrödinger). CB-20 was drawn in ChemDraw (Cambridge Software, Cambridge, MA). CB-20 was prepared using LigPrep (Maestro, Schrödinger). Ligand docking was employed to dock. Bound complexes were visualized using PyMOL (Schrödinger).

Statistical analysis

Data were analyzed using SPSS 19.0 software (SPSS Inc., Chicago, IL, USA). Student's t test or repeated measures ANOVA, followed by Fisher's least significant difference analysis for multiple comparisons, was used for data analysis according to different data types. $P < 0.05$ or $P < 0.01$ was considered statistically significant. Graphs were illustrated by GraphPad Prism (GraphPad Software Inc., La Jolla, CA, USA).

RESULTS

Identification of novel UT inhibitors

Based on HTVS and erythrocyte osmotic lysis assays, which were previously established [29], we modified and optimized the structure of UT inhibitors with a thienoquinoline core that was previously discovered. We discovered a novel compound, CB-20, that has UT-B inhibitory activity and a thienopyridine core and is chemically named 5-ethyl-2-methyl-3-amino-6-methylthieno [2,3-b]pyridine-2,5-dicarboxylate (Fig. 1a). The IC_{50} values of CB-20 on UT-B-facilitated urea transport were as follows (in μM): 2.01 ± 0.41 in mouse, 0.47 ± 0.19 in rat, and 1.29 ± 0.03 in human (Fig. 1b, c).

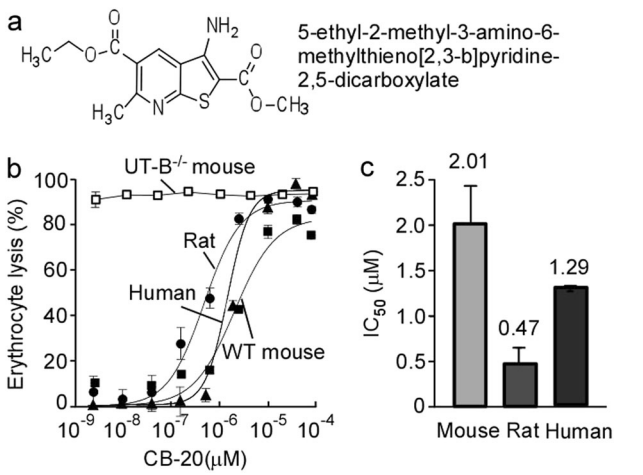

Fig. 1 Activity of CB-20 against mouse, rat, and human UT-B. **a** Chemical structure of CB-20. **b** Dose-dependent inhibitory activity of CB-20, as determined by an osmotic lysis assay in erythrocytes of UT-$B^{-/-}$ mice and wild-type mice, rats, and humans. **c** IC_{50} value of CB-20 on UT-B-facilitated urea transport

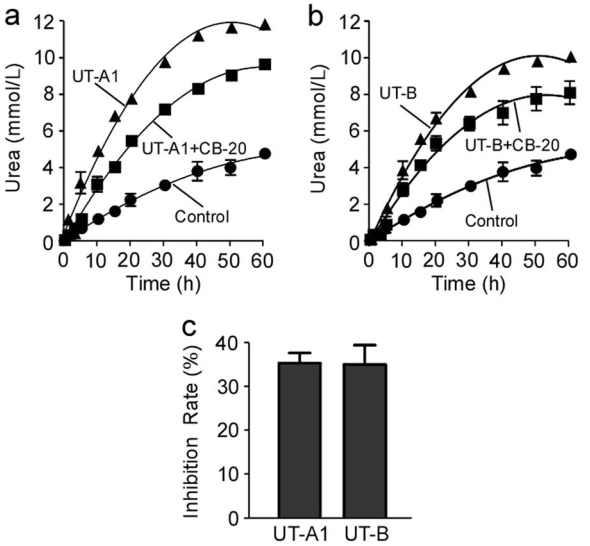

Fig. 2 Inhibition activity of CB-20 against human UT-A1- or UT-B-mediated urea transport in MDCK cells. **a** Inhibitory activity of CB-20 against UT-A1-mediated urea permeability. MDCK cells stably expressing human UT-A1 were treated with 10 μM forskolin (FSK). **b** Inhibitory activity of CB-20 against UT-B-mediated urea permeability. **c** The inhibition rate of CB-20 on UT-A1 and UT-B. Mean ± SEM, $n = 6$

CB-20 did not affect the transmembrane urea permeability in UT-B$^{-/-}$ erythrocytes. The maximal inhibition rate (I_{max}) of CB-20 on urea permeability in mouse, rat, and human erythrocyte lysis assays was greater than 80%.

Inhibition efficacy of CB-20 on human UT-A1 and UT-B

To identify the selectivity of UT inhibitors, lentiviral vectors expressing human UT-A1 and UT-B were constructed. The expression of UT-A1 and UT-B was confirmed by real-time PCR and immunofluorescence. The inhibitory activity of CB-20 against UT-A1 and UT-B was assayed in MDCK cell lines stably expressing UT-A1 and UT-B. As shown in Fig. 2a, b, the inhibition rates of CB-20 on UT-A1- and UT-B-mediated urea transport were 35.42% and 35.05%, respectively, which indicates that CB-20 had equal inhibitory activity against UT-A1 and UT-B (Fig. 2c).

Diuretic activity of single administration of CB-20 in vivo

To determine whether CB-20 has a diuretic effect in vivo, wild-type and UT-null mice [14] were put into metabolic cages to acclimate for 4 days and given a standard diet and free access to drinking water. CB-20 (100 mg/kg) was injected subcutaneously, and urine was collected every 2 h. As shown in Fig. 3, the urine volume of the wild-type mice increased after the administration of CB-20 for 2 h, and the diuretic effect peaked at 8 h. The diuretic effect lasted for almost 8 h and recovered to the basal level at 12 h after administration. Compared with that in the control group, the urine volume in the treated group was doubled at the eighth hour. However, there was no significant change in urine volume during 12 h after the administration of CB-20 to the UT$^{-/-}$ mice, which suggests that the diuretic effect of CB-20 is mainly due to the inhibition of UTs.

To confirm the diuretic activity of the CB-20 water conservation mechanism, SD rats fed ad libitum were observed in metabolic cages. Urine output significantly increased in a dose-dependent manner in rats subcutaneously administered with CB-20 at 25, 50, and 100 mg/kg compared with rats in the vehicle control group, as shown in Fig. 4a. Correspondingly, the urinary osmolality (Fig. 4b) and urea concentration (Fig. 4c) significantly decreased. Compared with those in the control group, the non-urea concentration

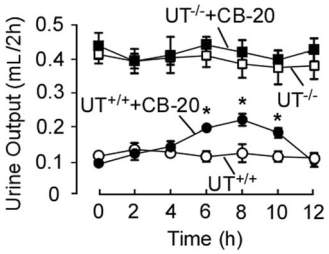

Fig. 3 Diuretic activity of a single subcutaneous injection of CB-20 in mice. After 2 h of urine collection, the UT$^{-/-}$ and WT mice were subcutaneously injected with 100 mg/kg CB-20 (time 0). Urine samples were collected every 2 h in metabolic cages. Urinary volume was measured by gravimetry. Mean ± SEM, $n = 6$, *$P < 0.05$ vs. control mice

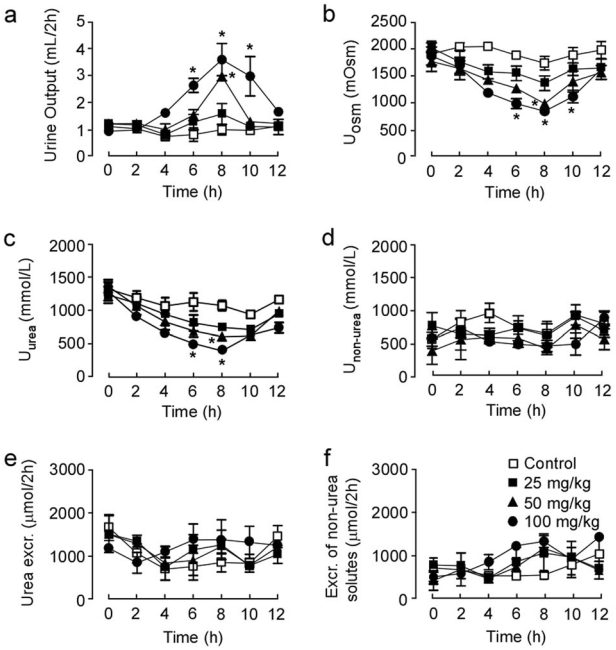

Fig. 4 Diuretic activity of a single subcutaneous injection of CB-20 in rats. After 2 h of urine collection, the rats were subcutaneously injected with 25, 50, or 100 mg/kg CB-20 (time 0). Urine samples were collected every 2 h in metabolic cages. **a** Urine output. **b** Urinary osmolality (U_{osm}). **c** Urinary urea concentration (U_{urea}). **d** Urine non-urea solute concentration ($U_{non\text{-}urea}$). **e** Urea excretion. **f** Excretion of non-urea solutes. Mean ± SEM, $n = 6$, *$P < 0.05$ vs. control rats

(Fig. 4d), urea excretion (Fig. 4e), and non-urea excretion (Fig. 4f) in the CB-20-treated groups were not significantly changed. The peak of the diuretic effect was 8 h after administration of CB-20 (100 mg/kg), and the duration of diuretic activity was ~6 h. The levels of urine output, urinary osmolality, and urinary urea concentration returned to the basal level at 12 h after CB-20 administration.

Diuretic activity of long-term administration of CB-20 in vivo

Clinically, diuretic drugs are usually used for long-term treatment, so we further observed the long-term diuretic effect of the UT inhibitor CB-20 in rats. CB-20 at 100 mg/kg was subcutaneously injected every 8 h. The solvent 2-hydroxypropyl-β-cyclodextrin was used as a vehicle control. The volume of urine started to increase on the first day of CB-20 administration and gradually

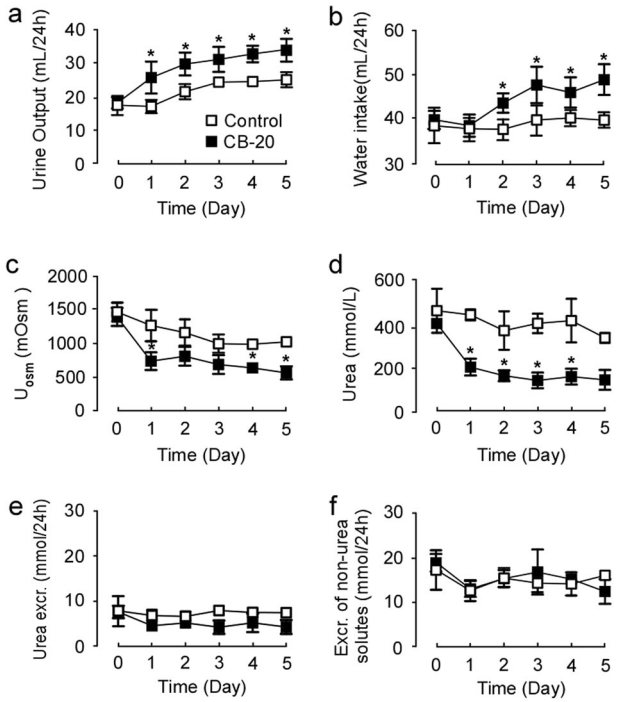

Fig. 5 Long-term diuretic activity of CB-20 in rats. Rats were subcutaneously injected with 100 mg/kg CB-20 just after a 24-h urine collection (time 0). Urine samples were collected every 24 h with metabolic cages. **a** Urine output. **b** Water intake. **c** Urinary osmolality (U_{osm}). **d** Urine urea concentration (U_{urea}). **e** Excretion of urea (urea excr.). **f** Excretion of non-urea solutes (non-urea excr.). Mean ± SEM, $n = 6$, $^*P < 0.05$ vs. control rats

Table 1. Blood and urinary chemistry in CB-20-treated rats

	Control	CB-20
Body weight, g	331.00 ± 9.42	333.50 ± 12.05
Urine output, mL/24 h	20.94 ± 1.99	35.55 ± 3.36*
Urinary osmolality, mOsm/kg H_2O	1100.67 ± 70.95	539.50 ± 57.63*
Serum osmolality, mOsm/kg H_2O	298.57 ± 12.42	294.25 ± 17.56
Osmolar excretion, mM/24 h	31.64 ± 1.66	19.44 ± 1.57
Urea excretion, mM/24 h	13.41 ± 2.32	14.40 ± 1.05
Urinary creatinine, μM	5213.10 ± 905.70	4353.21 ± 677.89
Serum creatinine, μM	32.25 ± 1.31	33.00 ± 1.34
Serum urea, mM	6.06 ± 0.38	5.74 ± 0.37
Serum GLU, mM	7.44 ± 0.75	6.56 ± 0.54
Serum T-CHO, mM	1.07 ± 0.08	0.80 ± 0.04
Serum TG, mM	1.04 ± 0.07	0.71 ± 0.08
Serum LDL-C, mM	0.29 ± 0.05	0.28 ± 0.03
Serum HDL-C, mM	0.38 ± 0.03	0.27 ± 0.02
Serum Na, mM	142.40 ± 27.03	137.62 ± 16.20
Serum K, mM	4.70 ± 0.43	4.37 ± 0.81
Serum Cl, mM	93.26 ± 5.81	96.64 ± 15.23
Urinary Na, mM	72.65 ± 11.32	43.02 ± 7.30*
Urinary K, mM	185.47 ± 7.35	138.03 ± 16.11*
Urinary Cl, mM	108.80 ± 8.12	96.15 ± 13.99*
Urinary urea, mM	441.70 ± 26.97	485.48 ± 69.98

TG triglyceride, *HDL-C* and *LDL-C* high- and low-density lipoprotein, *Glu* glucose, *Chol* cholesterol, *ALDO* aldosterone
Mean ± SEM, $n = 6$
$^*P < 0.05$ vs. control rats

reached a steady state on the second day until the fifth day. Compared with the solvent control group, the treated group had an obvious diuretic effect (Fig. 5a). The water intake of rats in the treated group began to increase on the second day, reached a steady state on the third day, and lasted until the fifth day (Fig. 5b). This result indicated that the water intake of rats increased after continuous administration of CB-20. The urinary osmolality and urea concentration in the treated group were significantly lower than those in the vehicle control group (Fig. 5c, d). However, the excretion of urea (Fig. 5e) and non-urea solutes (Fig. 5f) in the two groups remained similar.

Moreover, the levels of major electrolytes related to urine concentration in the urine and serum of rats were detected, and the results are shown in Table 1. Compared with those in the solvent control group, the urine levels of Na^+, K^+, and Cl^- in the CB-20 group were significantly decreased. However, there was no significant difference between the groups in the serum levels of Na^+, K^+, and Cl^-. The blood glucose, T-CHO, TG, LDL-C, and HDL-C were also not changed after the 5-day treatment with CB-20. The results indicate that CB-20 caused urea-selective diuresis without disturbing the electrolyte balance and normal metabolism.

Toxicity analysis of CB-20

To evaluate whether the inhibitory activity of CB-20 on UT was caused by its cytotoxicity and whether CB-20 could be used in vivo, a cell counting kit-8 (CCK-8) assay in MDCK cells was used to assay the toxicity of CB-20. Treatment with CB-20 at 80 μM for 72 h did not significantly reduce MDCK cell viability (Fig. 6a). The histopathological results showed no significant morphological abnormality in kidney or liver tissues after administration of CB-20 (Fig. 6b, c).

Rat pharmacokinetics

The mean plasma concentration–time profiles of CB-20 in rats are shown in Fig. 7. CB-20 was absorbed quickly after subcutaneous injection at a 100 mg/kg dose and reached the maximum concentration at 0.750 ± 0.433 h after administration. Then, the plasma concentrations decreased gently, and the plasma half-life ($t_{1/2}$) was 1.38 ± 0.11 h. The results demonstrated that CB-20 achieved good absorption in rats. At 8 h after subcutaneous administration, the mean plasma concentrations decreased below the lower limit of quantitation, which suggested that CB-20 underwent rapid and complete clearance from rat plasma.

Molecular docking of CB-20 with human UT-B

Computational docking was performed to propose the potential binding modes for CB-20 with human UT-B. As shown in Fig. 8a, CB-20 was bound to the cytoplasmic site of the UT-B channel. In the docked conformation (Fig. 8b), the planar scaffold of CB-20 is positioned near several hydrophobic residues, including Leu364, Val367, Phe71, and Val 69 (Fig. 8c), while the ethyloxy side chain was projected deeper into the cave surrounded by Thr177, Phe176, Val 175, and Tyr 124. In addition, there is a potential hydrogen bonding interaction between the amino group of CB-20 and the carbonyl oxygen in the side chain of Gln68, providing a relatively high affinity between CB-20 and the UT-B protein.

DISCUSSION

Previously, we found the phenylphthalazine compound PU_{1424}, which possessed inhibitory activity against both mouse and human UT-B in vitro but did not exhibit diuretic activity in vivo [32]. In this study, we identified a novel thienopyridine compound, CB-20, that had inhibitory activity against mouse, rat, and human

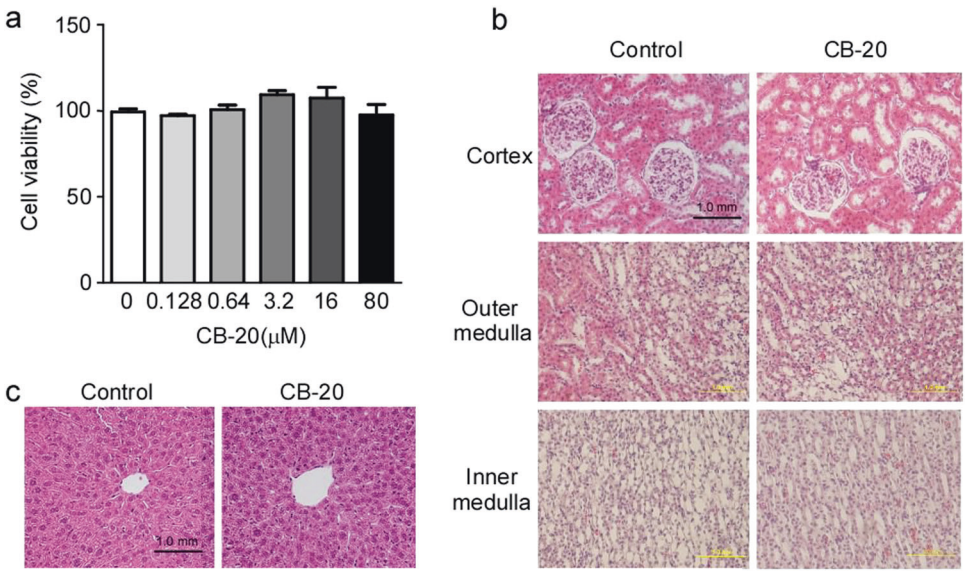

Fig. 6 Cellular toxicity of CB-20 and kidney and liver histology. **a** MDCK cells were cultured in the absence or presence of CB-20 at the indicated concentration for 72 h. Cell viability is shown as $OD_{450\,nm}$. **b** Kidney cortex, inner medulla, and outer medulla. **c** Liver ×400. Mean ± SEM, $n = 3$

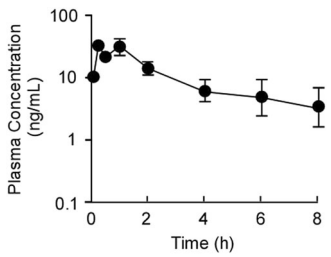

Fig. 7 Pharmacokinetics of CB-20 in rats. The plasma concentration of CB-20 in rats subcutaneously administered a 100 mg/kg dose. Data represent the mean ± SD ($n = 3$)

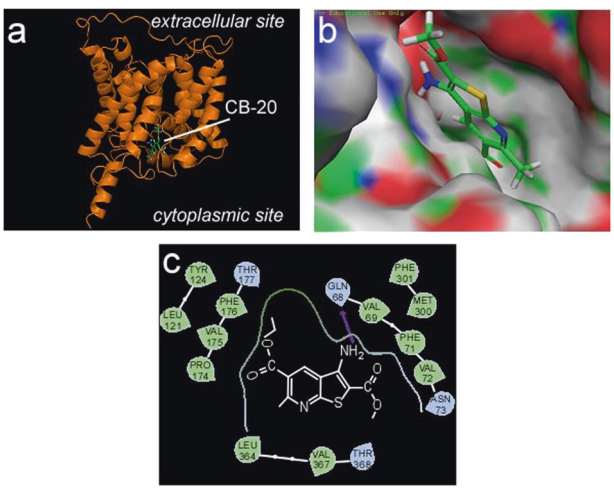

Fig. 8 Binding model of CB-20 with human UT-B (PDB: 6QD5) in silico. **a** Overall depiction. **b** Partial depiction. **c** Potential key residues of UT-B that interact with CB-20 (2D)

UT with micromolar potency, using HTVS and erythrocyte osmotic lysis assays. CB-20 had nearly equal inhibitory activity against both the UT-A1 and UT-B isoforms. Moreover, the urine volume of CB-20-treated mice was two times as high as that of control mice at the eighth hour after administration. There was no obvious effect of CB-20 in UT-null mice, which suggests that the diuretic effect of CB-20 is mainly due to the inhibition of UT.

Computational docking analysis showed that CB-20 was bound to the cytoplasmic site of the UT-B channel, which was similar to the binding mode of a previously reported active compound, UTBinh-14 [33], and was consistent with the result, showing the intracellular site of action of another active compound, PU-14 [28]. The data suggest that there is a relatively high affinity between CB-20 and the UT-B protein. The deduced binding sites for CB-20 with the human UT-B protein could be used to screen new classes of small molecules and to optimize CB-20 for discovering novel UT inhibitors with better pharmaceutical and biophysical characteristics.

To confirm the diuretic activity of the CB-20 water conservation mechanism, rats received a single subcutaneous administration of CB-20. Urine output significantly increased in a dose-dependent manner, and the urinary osmolality and urea concentration in treated rats were lower than those in vehicle control rats. When the rats were repeatedly subcutaneously injected with CB-20, the volume of urine started to increase on the first day and reached a steady state on the second day, accompanied by reduced urinary osmolality and urea concentration. All these results suggest that CB-20 caused urea-selective diuresis, which was consistent with the phenotypes of UT-knockout animals reported previously [12, 18, 20].

After multiple subcutaneous injections of CB-20 for 5 days, the excretion of urea and non-urea solutes did not change significantly, especially Na^+, K^+, and Cl^- levels. Moreover, metabolic parameters, including blood glucose, T-CHO, TG, LDL-C, and HDL-C levels, did not change after the 5 day treatment with CB-20. These results indicate that CB-20 caused urea-selective diuresis without disturbing the electrolyte balance and normal metabolism.

Toxicity analysis of CB-20 indicated that treatment with CB-20 at 80 μM for 48 h did not reduce MDCK cell viability. There was no

significant morphological abnormality in kidney or liver tissues 5 days after administration of CB-20 in rats. However, the side effects of CB-20 at diuretic doses should be determined.

Pharmacokinetics is a very important part of drug discovery, so we analyzed the plasma concentrations of CB-20 in rats. The results showed that CB-20 achieved good absorption and rapid, complete clearance from rat plasma. Although the plasma concentrations of CB-20 dropped rapidly, the diuretic activity remained longer, which indicates that CB-20 may quickly distribute to multiple tissues rapidly after being absorbed into the plasma. Another possibility is that CB-20 may break down into other metabolites under the action of metabolic enzymes, and that the metabolites play a diuretic role by inhibiting UT. However, this experiment only provided limited pharmacokinetic information about CB-20, and more studies in vivo and in vitro should be conducted to evaluate the drug-like properties of the compound in the future.

It has been reported that analogs of thienopyridine had other biological activities. Thienopyridine derivatives have significant antiproliferative activity against a range of human cancer tumor lines [34–37]. Methyl 6-methyl-3-[(3,4,5-trimethoxyphenyl) amino] thieno[2,3-b]pyridine-2-carboxylate has antiproliferative activity against four tumor cell lines, tubulin polymerization inhibitory activity, anti-drug-resistant activity, and apoptosis-inducing activity [38]. In addition, a series of thienopyridine compounds can bind to the HIV-1 transactivation response hairpin, a *cis*-acting HIV genomic element, which has long been an important model system for developing compounds to target RNA [39].

In summary, we found a thienopyridine UT inhibitor, CB-20, using HTVS and erythrocyte osmotic lysis assays combined with a screening model. CB-20 exerted diuretic activity by inhibiting both UT-A1 and UT-B without disturbing the electrolyte balance and normal metabolism. CB-20 also possessed good absorption and rapid clearance from rat plasma. Based on further research and development, CB-20 might be developed as a novel diuretic.

ACKNOWLEDGEMENTS

This work was supported by the National Natural Science Foundation of China (grants 81500535, 81620108029, and 81330074), the Leading Academic Discipline Project of Beijing Education Bureau (BMU20110254), and the Natural Science Foundation of Chongqing Science and Technology Commission (cstc2015jcyjA10036).

AUTHOR CONTRIBUTIONS

ML, RTL, and BXY conceived and designed the experiments. ML performed the experiments. YZ and SZ analyzed the data. YX, SYW, BWL, and JHR contributed reagents/materials/analysis tools. ML and BXY wrote the paper.

REFERENCES

1. Jentzer JC, DeWald TA, Hernandez AF. Combination of loop diuretics with thiazide-type diuretics in heart failure. J Am Coll Cardiol. 2010;56:1527–34.
2. Moser M, Feig PU. Fifty years of thiazide diuretic therapy for hypertension. Arch Intern Med. 2009;169:1851–6.
3. Mann SJ. The silent epidemic of thiazide-induced hyponatremia. J Clin Hypertens. 2008;10:477–84.
4. Plavinik FL, Rodrigues CI, Zanella MT, Ribeiro AB. Hypokalemia, glucose intolerance, and hyperinsulinemia during diuretic therapy. Hypertension. 1992;19: II26–9.
5. Verdecchia P, Reboldi G, Angeli F, Borgioni C, Gattobigio R, Filippucci L, et al. Adverse prognostic significance of new diabetes in treated hypertensive subjects. Hypertension. 2004;43:963–9.
6. Franse LV, Pahor M, Di Bari M, Shorr RI, Wan JY, Somes GW, et al. Serum uric acid, diuretic treatment and risk of cardiovascular events in the Systolic Hypertension in the Elderly Program (SHEP). J Hypertens. 2000;18:1149–54.
7. O'Brien E, Barton J, Nussberger J, Mulcahy D, Jensen C, Dicker P, et al. Aliskiren reduces blood pressure and suppresses plasma renin activity in combination with a thiazide diuretic, an angiotensin-converting enzyme inhibitor, or an angiotensin receptor blocker. Hypertension. 2007;49:276–84.
8. Mason JM, Dickinson HO, Nicolson DJ, Campbell F, Ford GA, Williams B. The diabetogenic potential of thiazide-type diuretic and beta-blocker combinations in patients with hypertension. J Hypertens. 2005;23:1777–81.
9. Yamamura Y, Ogawa H, Yamashita H, Chihara T, Miyamoto H, Nakamura S, et al. Characterization of a novel aquaretic agent, OPC-31260, as an orally effective, nonpeptide vasopressin V2 receptor antagonist. Br J Pharmacol. 1992;105: 787–91.
10. Thibonnier M, Coles P, Thibonnier A, Shoham M. The basic and clinical pharmacology of nonpeptide vasopressin receptor antagonists. Annu Rev Pharmacol Toxicol. 2001;41:175–202.
11. Uchida S, Sohara E, Rai T, Ikawa M, Okabe M, Sasaki S. Impaired urea accumulation in the inner medulla of mice lacking the urea transporter UT-A2. Mol Cell Biol. 2005;25:7357–63.
12. Fenton RA, Flynn A, Shodeinde A, Smith CP, Schnermann J, Knepper MA. Renal phenotype of UT-A urea transporter knockout mice. J Am Soc Nephrol. 2005;16:1583–92.
13. Li X, Chen G, Yang B. Urea transporter physiology studied in knockout mice. Front Physiol. 2012;3:217.
14. Jiang T, Li Y, Layton AT, Wang W, Sun Y, Li M, et al. Generation and phenotypic analysis of mice lacking all urea transporters. Kidney Int. 2017;91:338–51.
15. Shayakul C, Hediger MA. The SLC14 gene family of urea transporters. Pflug Arch. 2004;447:603–9.
16. Fenton RA, Stewart GS, Carpenter B, Howorth A, Potter EA, Cooper GJ, et al. Characterization of mouse urea transporters UT-A1 and UT-A2. Am J Physiol Ren Physiol. 2002;283:F817–25.
17. Doran JJ, Klein JD, Kim YH, Smith TD, Kozlowski SD, Gunn RB, et al. Tissue distribution of UT-A and UT-B mRNA and protein in rat. Am J Physiol Regul Integr Comp Physiol. 2006;290:R1446–59.
18. Yang B, Bankir L, Gillespie A, Epstein CJ, Verkman AS. Urea-selective concentrating defect in transgenic mice lacking urea transporter UT-B. J Biol Chem. 2002;277:10633–7.
19. Fenton RA, Knepper MA. Urea and renal function in the 21st century: insights from knockout mice. J Am Soc Nephrol. 2007;18:679–88.
20. Fenton RA, Chou CL, Stewart GS, Smith CP, Knepper MA. Urinary concentrating defect in mice with selective deletion of phloretin-sensitive urea transporters in the renal collecting duct. Proc Natl Acad Sci USA. 2004;101:7469–74.
21. Lei T, Zhou L, Layton AT, Zhou H, Zhao X, Bankir L, et al. Role of thin descending limb urea transport in renal urea handling and the urine concentrating mechanism. Am J Physiol Ren Physiol. 2011;301:F1251–9.
22. Esteva-Font C, Phuan PW, Anderson MO, Verkman AS. A small molecule screen identifies selective inhibitors of urea transporter UT-A. Chem Biol. 2013;20: 1235–44.
23. Knepper MA, Miranda CA. Urea channel inhibitors: a new functional class of aquaretics. Kidney Int. 2013;83:991–3.
24. Sands JM. Urea transporter inhibitors: en route to new diuretics. Chem Biol. 2013;20:1201–2.
25. Tsuchiya Y, Vidaurre D, Toh S, Hanada A, Nambara E, Kamiya Y, et al. A small-molecule screen identifies new functions for the plant hormone strigolactone. Nat Chem Biol. 2010;6:741–9.
26. Yang B, Bankir L. Urea and urine concentrating ability: new insights from studies in mice. Am J Physiol Ren Physiol. 2005;288:F881–96.
27. Esteva-Font C, Anderson MO, Verkman AS. Urea transporter proteins as targets for small-molecule diuretics. Nat Rev Nephrol. 2015;11:113–23.
28. Li F, Lei T, Zhu J, Wang W, Sun Y, Chen J, et al. A novel small-molecule thienoquinolin urea transporter inhibitor acts as a potential diuretic. Kidney Int. 2013;83:1076–86.
29. Li M, Tou WI, Zhou H, Li F, Ren H, Chen CY, et al. Developing hypothetical inhibition mechanism of novel urea transporter B inhibitor. Sci Rep. 2014;4:5775.
30. Levin MH, de la Fuente R, Verkman AS. Urearetics: a small molecule screen yields nanomolar potency inhibitors of urea transporter UT-B. FASEB J. 2007;21: 551–63.
31. Mazeron P, Didelon J, Muller S, Stoltz JF. A theoretical approach of the measurement of osmotic fragility of erythrocytes by optical transmission. Photochem Photobiol. 2000;72:172–8.
32. Ran JH, Li M, Tou WI, Lei TL, Zhou H, Chen CY, et al. Phenylphthalazines as small-molecule inhibitors of urea transporter UT-B and their binding model. J Am Soc Nephrol. 2016;37:973–83.
33. Yao C, Anderson MO, Zhang J, Yang B, Phuan PW, Verkman AS. Triazolothienopyrimidine inhibitors of urea transporter UT-B reduce urine concentration. J Am Soc Nephrol. 2012;23:1210–20.
34. Feng L, Reynisdottir I, Reynisson J. The effect of PLC-gamma2 inhibitors on the growth of human tumour cells. Eur J Med Chem. 2012;54:463–9.

35. Hung JM, Arabshahi HJ, Leung E, Reynisson J, Barker D. Synthesis and cytotoxicity of thieno[2,3-b]pyridine and furo[2,3-b]pyridine derivatives. Eur J Med Chem. 2014;86:420–37.
36. Deng XQ, Wang HY, Zhao YL, Xiang ML, Jiang PD, Cao ZX, et al. Pharmacophore modelling and virtual screening for identification of new Aurora-A kinase inhibitors. Chem Biol Drug Des. 2008;71:533–9.
37. Zhou R, Huang WJ, Guo ZY, Li L, Zeng XR, Deng YQ, et al. Molecular mechanism of hepatocellular carcinoma-specific antitumor activity of the novel thienopyridine derivative TP58. Oncol Rep. 2012;28:225–31.
38. Romagnoli R, Baraldi PG, Kimatrai Salvador M, Preti D, Aghazadeh Tabrizi M, Bassetto M, et al. Synthesis and biological evaluation of 2-(alkoxycarbonyl)-3-anilinobenzo[b]thiophenes and thieno[2,3-b]pyridines as new potent anticancer agents. J Med Chem. 2013;56:2606–18.
39. Abulwerdi FA, Shortridge MD, Sztuba-Solinska J, Wilson R, Le Grice SF, Varani G, et al. Development of small molecules with a noncanonical binding mode to HIV-1 Trans Activation Response (TAR) RNA. J Med Chem. 2016;59:11148–60.